# Reverse Flood Routing in Rivers Using Linear and Nonlinear Muskingum Models

Meisam Badfar[1]; Reza Barati, Ph.D.[2]; Emrah Dogan[3]; and Gokmen Tayfur[4]

**Abstract:** One of the key factors for flood modeling and control is the flood hydrograph, which is not always available due to lack of flood discharge observations. In reverse flow routing, hydraulic or hydrological calculations are performed from the downstream end to the upstream end. In the present study, a reverse flood routing approach is developed based on the Muskingum model. The storage function is conceptualized as linear and five different nonlinear forms. The Euler and the fourth-order Runge–Kutta numerical methods are used for solving the storage models. The shuffled complex evolution (SCE) algorithm is used for optimization of the flood routing parameters. The models are calibrated and validated with theoretical and actual hydrographs. The results indicate that the proposed methodology could substantially (up to almost 82%) improve comparison with observed inflows. The practical applicability of the proposed methodology is also validated in real river systems. **DOI: 10.1061/(ASCE)HE.1943-5584.0002088.** 

**Author keywords:** Reverse flow routing; Muskingum models; Numerical schemes; Parameter estimation; Optimization algorithm.

## Introduction

Flood routing is a mathematical process for the temporal prediction of volume change, velocity, flow rates, and shape of a flood wave in a river reach. It is important for the river engineering, flood control, river conservation, and modeling of flow in reservoirs and over spillways (Chow et al. 1988; Brutsaert 2005; Sivapragasam et al. 2008; Szymkiewicz 2010; Battjes and Labeur 2017). Two general approaches can be considered for the classification of flood routing modeling. The first approach utilizes hydrologic, hydraulic, and black box models. Hydrologic models are based on the storage-continuity equation; hydraulic models are based on the numerical solution of Saint-Venant equations; and black box models use historical data for developing and training the models. The second approach utilizes flood routing techniques as distributed models (e.g., Akbari et al. 2012), semidistributed models (e.g., Perumal and Sahoo 2007), and lumped models (e.g., Koussis 2009). Lumped models can only predict a hydrograph at one section of a river reach, while distributed models can predict hydrographs for different sections along a river reach.

Forward (direct) flood routing predicts a hydrograph at a downstream hydrometric station, whereas reverse flood routing is performed from downstream to the top of the river reach. Reverse flow routing provides the necessary information for the design of hydraulic structures.

There have been several applications of implicit and explicit finite difference schemes for reverse flood routing based on solving Saint-Venant equations under different hydraulic conditions (Eli et al. 1974; Szymkiewicz 1993; Zoppou 1999; Dooge and Bruen 2005; Price et al. 2006; Bruen and Dooge 2007; Artichowicz and Szymkiewicz 2009; Abdulwahid and Kadhim 2013; Spada et al. 2017). On the other hand, there have been some applications of simple approaches for reverse flood routing including: (1) level pool routing (Zoppou 1999; Artichowicz and Szymkiewicz 2009; D'Oria et al. 2012), (2) Bayesian geostatistical approach (D'Oria and Tanda 2012; D'Oria et al. 2014), and (3) hybrid approaches of a routing model and a optimization algorithm (Saghafian et al. 2015; Zucco et al. 2015). Low accuracy and sensitivity of the results to calibrated parameters are the main drawbacks of these approaches. However, these approaches can perform inverse hydrograph routing with numerical stability.

Although there are studies using the Muskingum model for forward flood routing (e.g., Barati 2011, 2013; Niazkar and Afzali 2017; Kang et al. 2017; Ayvaz and Gurarslan 2017; Vatankhah 2014; Ehteram et al. 2018), the application of this model for reverse flood routing is few. Das (2009) studied the performance of the Muskingum model for reverse flood routing. He used the Lagrange multipliers for parameter optimization. The results revealed the need of the Muskingum model calibration for reverse flood routing. Sadeghi and Singh (2010) developed an analytical procedure through which the outflow hydrographs could be calculated for each subwatershed/area using the Muskingum hydrologic routing model and the Area-curve number (CN) factor. Koussis et al. (2012) compared the reverse Muskingum routing model against a reverse-solution method of the Saint-Venant equations of the flood wave motion and they found that the Muskingum model performed equally well at a fraction of the computing effort. Existing reverse flood routing studies based on the Muskingum model have been mostly focused on the linear model for prediction of single-peak hydrographs and tested against artificial hydrographs. These studies, as with the optimization model, used the genetic algorithm (GA) or variants of GA algorithms that have local minima problem.

[1]Ph.D. Candidate, Faculty of Engineering, Dept. of Civil Engineering, Sakarya Univ., Kemalpaşa Esentepe Kampüsü, Üniversite Cd., Serdivan/Sakarya 54050, Turkey. ORCID: https://orcid.org/0000-0002-9687-4102. Email: Meisam.Badfar@gmail.com

[2]Head of Applied Research Group at Water Authority, Khorasan Razavi Water Authority, District 1, Mashhad, Razavi Khorasan Province 9185916196, Iran (corresponding author). ORCID: https://orcid.org/0000-0003-2362-2227. Email: r88barati@gmail.com

[3]Professor, Dept. of Civil Engineering, Sakarya Univ., Kemalpaşa Esentepe Kampüsü, Üniversite Cd., Serdivan/Sakarya 54050, Turkey. Email: emrahd@sakarya.edu.tr

[4]Professor, Dept. of Civil Engineering, Izmir Institute of Technology, İzmir Yüksek Teknoloji Enstitüsü Gülbahçe Mah, Urla/İzmir 35430, Turkey. Email: gokmentayfur@iyte.edu.tr

Note. This manuscript was submitted on May 28, 2020; approved on January 21, 2021; published online on March 25, 2021. Discussion period open until August 25, 2021; separate discussions must be submitted for individual papers. This paper is part of the ***Journal of Hydrologic Engineering***, © ASCE, ISSN 1084-0699.

Also, these studies mostly used the simple Euler or modified Euler methods for solving the Muskingum storage models.

In previous studies, many researchers tested the shuffled complex evolution (SCE) algorithm on a variety of models with positive results. Examples include the calibration of parameters of the rainfall-runoff models (Duan et al. 1992; Sorooshian et al. 1993; Yapo et al. 1996); the finite-element groundwater flow model (Contractor and Jenson 2000); the Soil and Water Assessment Tool (SWAT) (Eckhardt and Arnold 2001); the hydrologic and water quality model (van Griensven and Bauwens 2003); the linear reservoir flood model (Cheng and Wang 2002); the MIKE SHE hydrological modeling system (Mertens et al. 2004); and the groundwater flow modeling tools (Eusuff and Lansey 2004). To summarize, the SCE algorithm is able to cope very well with highly nonsmooth objective function surfaces.

Vatankhah (2014) used different explicit numerical solution methods for the forward (direct) flood routing. In the present research, the fourth-order Runge–Kutta method, which is known as the most accurate and widely used numerical method for solving the initial value problems, is used for solving the linear and nonlinear storage models. Furthermore, the SCE algorithm, which has no local minimum problem, is adopted for optimization of the reverse flood routing parameters. Six storage equations [Eqs. (2)–(7)] are applied for routing a triangular, a single-peak, a double-peak, and multipeak flood hydrographs. Moreover, the proposed methodology was used for calibrating and validating a real case event. As will be shown, the proposed methodology substantially improved the fit to observed inflows considered from previous studies.

The subsequent sections include descriptions of the Muskingum routing models, the proposed reverse flood routing procedure, the details of the SCE algorithm, and a discussion of the models' results and conclusions.

## Muskingum Routing Models

The Muskingum model is a lumped-hydrologic flood routing model that uses the following hydrologic budget equation (McCarthy 1938):

$$\frac{ds}{dt} = I - O \tag{1}$$

where $O$ = outflow discharge; $I$ = inflow discharge; $t$ = time; and $S$ = storage.

Channel storage is commonly modeled by using either a linear storage equation or nonlinear equations that relates the storage to the inflow and outflow with some model parameters. In the linear Muskingum model (LN), the following storage equation is used:

$$S = K[XI + (1 - X)O] \tag{2}$$

where $K$ = storage-time constant for the river reach ($T$); and $X$ = dimensionless weighting factor.

It is not uncommon to observe a nonlinear relationship between weighted flow and storage volume (Tung 1985). For this purpose, several nonlinear Muskingum models were suggested, as follows:

First nonlinear model (NL1; Chow 1959):

$$\mathrm{S} = \mathrm{K}[\mathrm{XI} + (1 - \mathrm{X})\mathrm{O}]^{\mathrm{m_1}} \tag{3}$$

Second nonlinear model (NL2; Gill 1978):

$$\mathrm{S} = \mathrm{K}[\mathrm{XI}^{\mathrm{m_1}} + (1 - \mathrm{X})\mathrm{O}^{\mathrm{m_1}}] \tag{4}$$

Third nonlinear model (NL3; Gavilan and Houck 1985):

$$\mathrm{S} = \mathrm{K}[\mathrm{XI}^{\mathrm{m_1}} + (1 - \mathrm{X})\mathrm{O}^{\mathrm{m_2}}] \tag{5}$$

Fourth nonlinear model (NL4; Easa 2014):

$$\mathrm{S} = \mathrm{K}[\mathrm{XI}^{\mathrm{m_1}} + (1 - \mathrm{X})\mathrm{O}^{\mathrm{m_1}}]^{\mathrm{m_2}} \tag{6}$$

Fifth nonlinear model (NL5; Easa et al. 2014; Vatankhah 2015):

$$\mathrm{S} = \mathrm{K}[\mathrm{XI}^{\mathrm{m_1}} + (1 - \mathrm{X})\mathrm{O}^{\mathrm{m_2}}]^{\mathrm{C}} \tag{7}$$

In Eqs. (3)–(7), $m_1$, $m_2$, and $C$ are exponential parameters that were considered as the routing parameters. The exponential parameters were added to the linear model to provide additional degree(s) of freedom and to better model the relationship between storage volume and weighted flow.

## Reverse Flood Routing Procedure

From the continuity equation [Eq. (1)], the rate of change of the storage volume with respect to time is stated by an ordinary first-order differential equation. There is no analytical solution for this equation, and thus, is solved by numerical solution techniques. In the present study, for reverse flood routing, two explicit numerical solution methods are described (Badfar 2015).

### *Euler Method*

The solution of the reverse flood routing model using the Euler method (EM) for Eq. (3) is summarized as follows:

Step 1: Assume values for the three hydrologic parameters ($K$, $X$, and $m_1$).

Step 2: Calculate the storage value by Eq. (3). It should be noted that the initial calculated inflow is considered to be the same as the initial observed outflow.

Step 3: Calculate the rate of change of storage volume as:

$$\frac{ds}{dt} = \frac{1}{X}\left(\frac{S_i}{K}\right)^{\frac{1}{m_1}} - \frac{1}{X}O_i \tag{8}$$

Step 4: Calculate the storage at previous time step as:

$$S_i = S_{i+1} - \Delta S_{i+1} \tag{9}$$

Step 5: Calculate the inflow at previous time step as:

$$I_i = \frac{1}{X}\left(\frac{S_i}{K}\right)^{\frac{1}{m_1}} - \frac{1 - X}{X}O_i \tag{10}$$

Step 6: Steps 3–5 are repeated for all $N$ time steps.

A similar procedure is used for other storage equations [Eqs. (2) and (4)–(7)] of the Muskingum model.

### *Fourth-Order Runge–Kutta Method*

The solution of the reverse flood routing model using the fourth-order Runge–Kutta (FORK) method for Eq. (3) is summarized as follows:

Step 1: Assume values for the three hydrologic parameters ($K$, $X$, and $m_1$).

Step 2: Calculate the storage value by Eq. (3). It should be noted that the initial calculated inflow is considered to be the same as the initial observed outflow.

Step 3: Calculate the rate of change of storage volume, after obtaining FORK coefficients, as follows:

$$K_1(i) = \frac{1}{X}\left(\frac{S_i}{K}\right)^{\frac{1}{m1}} - \frac{1}{X}O_i \tag{11}$$

$$K_2(i) = \frac{1}{X}\left(\frac{S_i + \frac{1}{2}K_1(i)dt}{K}\right)^{\frac{1}{m1}} - \frac{1}{X}\left(\frac{O_i + O_{i-1}}{2}\right) \tag{12}$$

$$K_3(i) = \frac{1}{X}\left(\frac{S_i + \frac{1}{2}K_2(i)dt}{K}\right)^{\frac{1}{m1}} - \frac{1}{X}\left(\frac{O_i + O_{i-1}}{2}\right) \tag{13}$$

$$K_4(i) = \frac{1}{X}\left(\frac{S_i + K_3(i)dt}{K}\right)^{\frac{1}{m1}} - \frac{1}{X}(O_{i-1}) \tag{14}$$

$$\frac{ds}{dt}(i) = \frac{1}{6}(K_1(i) + 2K_2(i) + 2K_3(i) + K_4(i)) \tag{15}$$

$$\frac{ds}{dt} = \frac{1}{X}\left(\frac{S_i}{K}\right)^{\frac{1}{m1}} - \frac{1}{X}O_i \tag{16}$$

Step 4: Calculate the storage at previous time step using Eq. (9).
Step 5: Calculate the inflow for at previous time step as:

$$I_i = \frac{1}{X}\left(\frac{S_i}{K}\right)^{\frac{1}{m1}} - \frac{1-X}{X}O_i \tag{17}$$

Step 6: Steps 3–5 are repeated for all $N$ time steps.

A similar procedure is used for other storage equations [Eqs. (2) and (4)–(7)] of the Muskingum model.

## Shuffled Complex Evolution Algorithm

The SCE algorithm incorporates the best features from several deterministic and stochastic methods, wherein a global search algorithm is used to minimize a single function using only functional values (Duan et al. 1992). The SCE algorithm is extensively used in watershed model calibration and other areas of hydrology such as soil erosion, subsurface hydrology, remote sensing, and land surface modeling. It has been found to be generally robust and effective, and also utilizes a flexible and efficient search algorithm for a broad class of problems (Duan 2003).

The SCE algorithm works on the basis of four concepts (Duan et al. 1992, 1993; Gupta et al. 1999): (1) blend of deterministic and stochastic approaches, (2) systematic evolution of a complex of points, (3) competitive evolution, and (4) complex shuffling. The procedure of the SCE algorithm was presented in Duan et al. (1992) and Duan et al. (1993) and the flowchart is presented here for completeness (Fig. 1).

Four stopping criteria are used in the SCE algorithm at each generation:

- Difference between best and worst function evaluation in population is smaller than the tolerance (e.g., 0.001);
- Maximum difference between the coordinates of the vertices in simplex is less than the tolerance (e.g., 0.001);
- Maximum number of function evaluations or iterations are reached (e.g., 2,500); and
- Maximum duration of optimization is reached (e.g., 30 s).

The SCE algorithm is controlled by some algorithmic parameters including:

- The number of points in a complex, $m$ ($m \geq 2$);
- The number of points in a subcomplex, $q$ ($2 \leq q \leq m$);
- The number of complexes, $p$ ($p \geq 1$);

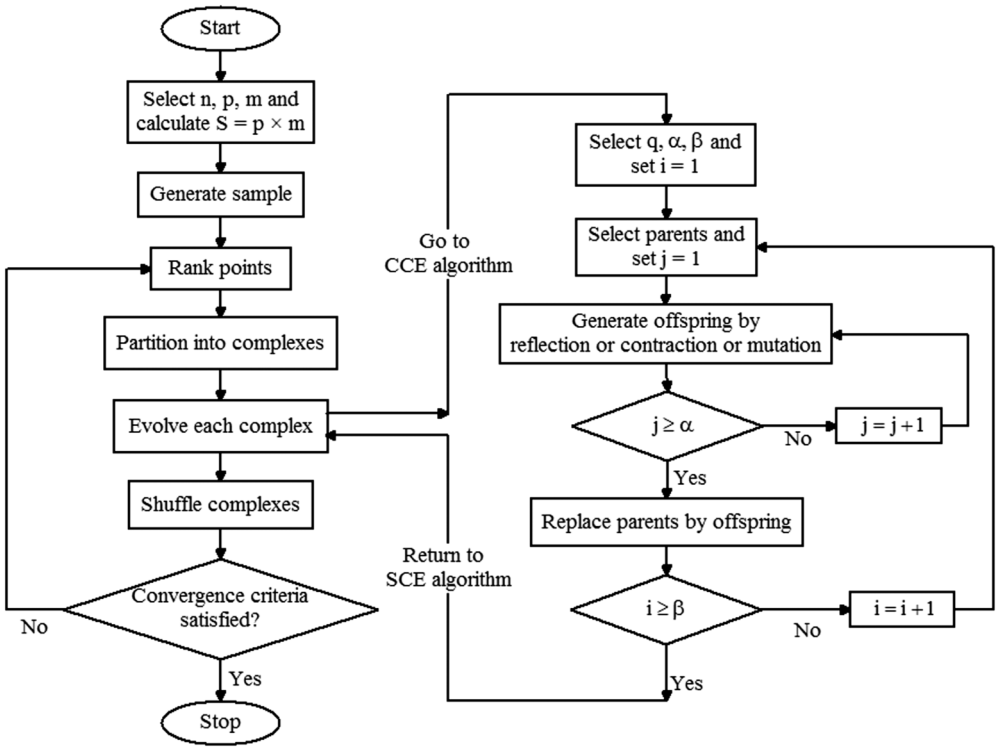


**Fig. 1.** Flowchart of the SCE algorithm. Note: $m$ = number of points in each complex; $p$ = number of complexes; $n$ = number of decision variables; $S$ = sample size; $q$ = number of points in a subcomplex; $\alpha$ = number of consecutive offspring generated by a subcomplex; and $\beta$ = number of evolution steps taken by each complex. (Data from Duan et al. 1992.)



J. Hydrol. Eng., 2021, 26(6): 04021018

**Table 1.** Estimated parameters and evaluation criteria values of Muskingum models for triangular flood data

| Routing parameters or criteria | Storage model | | | | | | | | Saghafian et al. (2015) |
|---|---|---|---|---|---|---|---|---|---|
| | LN | | NL1 | | | | | | |
| | EM | FORK | EM | FORK | NL2 | NL3 | NL4 | NL5 | |
| $K$ | 15.8077 | 26.3223 | 166.5695 | 118.8873 | 96.8812 | 391.7746 | 124.2356 | 2,677.78 | — |
| $X$ | 0.3526 | 0.2646 | 0.3297 | 0.2403 | 0.2487 | 0.0362 | 0.2451 | 0.0004 | — |
| $m_1$ | — | — | 0.5979 | 0.7437 | 0.7760 | 0.8625 | 0.9014 | 0.7521 | — |
| $m_2$ | — | — | — | — | — | 0.5077 | 0.8123 | 0.0270 | — |
| $C$ | — | — | — | — | — | — | — | 8.5204 | — |
| SSE ($m^3 \cdot s^{-1}$) | 280 | 280 | 146 | 134 | 143 | 106 | 125 | **96** | 534 |
| SAD ($m^3 \cdot s^{-1}$) | 89 | 89 | 60 | 57 | 60 | 50 | 55 | **48** | 864 |
| DBP ($m^3 \cdot s^{-1}$) | **3.0** | **3.0** | 3.6 | 4.1 | 4.3 | 4.9 | 4.2 | 5.6 | 8.9 |
| DBTP | **0** | **0** | **0** | **0** | **0** | **0** | **0** | **0** | 3 |

Note: Bold values indicate the minimum value (better performance) among different approaches.

- The number of consecutive offspring generated by each subcomplex, $\alpha$ ($\alpha \geq 1$); and
- The number of evolution steps taken by each complex, $\beta(\beta \geq 1)$.

The suitable values for these parameters as a function of the number of parameters to be optimized are: $m = (2n + 1)$; $q = (n + 1)$; $\alpha = 1$; and $\beta = (2n + 1)$ (Duan et al. 1994).

## Routing Scenarios and Performance Evaluation Criteria

By considering the described methodology, three main objectives will be achieved: (1) evaluation of the performance of EM and FORK, (2) comparison of the performance of the six proposed Muskingum storage equations, and (3) an assessment of the efficiency of the SCE algorithm. In order to achieve these objectives, four different flood events (represented by a triangular flood hydrograph, a single-peak flood hydrograph, a two-peak flood hydrograph, and a multipeak flood hydrograph) are used. Various relationships between storage volume and weighted flows are considered in the calibration step and two flood events in a river reach are used for model calibration and validation. The EM and FORK were compared using the results of the LN storage equation and NL1. As will be shown, the FORK has a better performance than the EM, and therefore, other four nonlinear models (NL2–NL5) are only simulated using the FORK as the numerical simulation scheme.

The objective function for the optimal estimation of flood routing parameters of the Muskingum storage equations is to minimize the sum of square error (SSE) between computed $\hat{I}_\iota$ and observed $I_i$ inflows as follows:

$$\min SSE = \sum_{i=1}^{N} \{I_i - \hat{I}_\iota\}^2 \tag{18}$$

To evaluate and compare the performances of the models, three performance evaluation criteria are used, as follows:

1. The sum of absolute difference (SAD) between observed and computed values of inflow:

$$SAD = \sum_{i=1}^{N} |I_i - \hat{I}_\iota| \tag{19}$$

2. The difference between the peak (DBP) discharges of the computed and observed inflows:

$$DBP = |I_{pi} - \widehat{I_{pc}}| \tag{20}$$

3. The difference between the time to the peak (DBTP) of the calculated and observed inflows:

$$DBTP = \frac{|T_{pi} - T_{pc}|}{\Delta t} \tag{21}$$

In Eqs. (18)–(21), $I_i$, $\hat{I}_\iota$ respectively are the observed and calculated inflow rates at the $i$th time, $N$ is the number of data, $I_{pi}$ is the peak flow of the observed upstream hydrograph, $I_{pc}$ is the peak flow of the calculated upstream hydrograph, $T_{pi}$ is the time of the peak flow of the observed upstream hydrograph, $T_{pc}$ is the time of the peak flow of the calculated upstream hydrograph, and $\Delta t$ is the time s t ep. All described criteria are the measures of the accuracy of a routing model with the optimum value at 0.

## Results and Discussion

### *First Case Study: Triangular Flood Hydrograph*

Saghafian et al. (2015) used a triangular inflow hydrograph in a rectangular channel with length of 4,500 m, a bed width of 60 m, a bed slope of 0.01, and a Manning roughness coefficient of 0.035. They applied the kinematic wave approach using a time step of 3 min for simulation of the upstream hydrograph. This flood event has a linear relationship between storage volume and weighted flow (Saghafian et al. 2015).

The results of the optimized flood routing parameters using the Muskingum models (LN, NL1–NL5) are summarized in Table 1. Comparison of routed upstream hydrographs of the present study, Saghafian et al. (2015), and observed recorded inflow data are depicted in Fig. 2. The simulated inflow hydrographs are performed fairly well by the reverse flood routing as shown in this figure.

The values of the evaluation criteria for different Muskingum models together with those of Saghafian et al. (2015) are also summarized in Table 1. As it is clear, all Muskingum models have a better performance than the result of Saghafian et al. (2015) in terms of SSE, SAD, DBP, and DBTP. The improvement of the performance of the Muskingum models is at least 48% (i.e., 91% decreasing SSE value) for the linear model, and the most improvement of the accuracy is 82% (i.e., 456% decreasing SSE value) for the NL5 in term of SSE value. Moreover, the simulated inflow hydrograph by Saghafian et al. (2015) was a nonsmooth curve (e.g., fluctuations of discharge values in rising and/or falling limbs

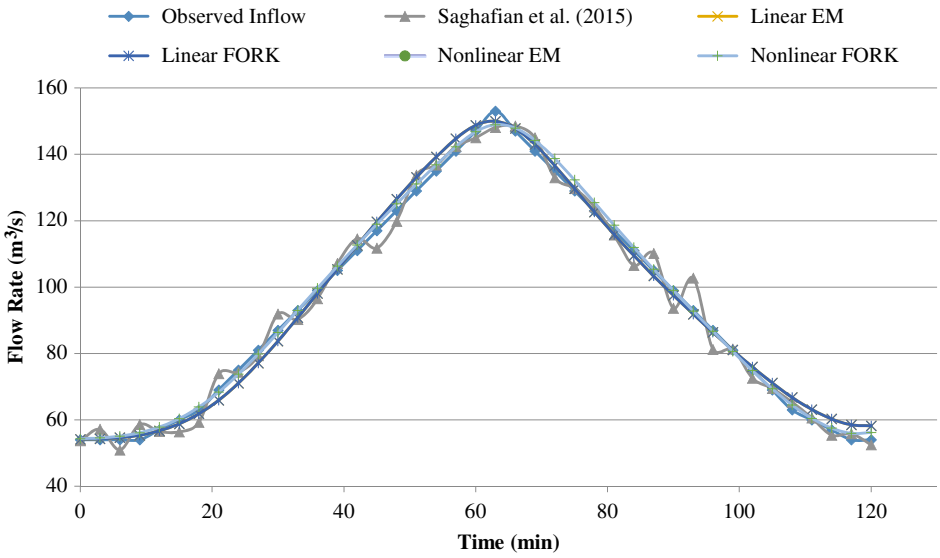


**Fig. 2.** Comparison of routed upstream hydrographs of the present study and Saghafian et al. (2015) for triangular flood data.

of the flood hydrograph), as opposed to the hydrographs obtained in this study (Fig. 2).

The comparisons of the results of the EM and FORK for linear and first nonlinear Muskingum models (Table 1) indicate that both numerical scheme have the same performance for the linear model, while FORK has slightly better results in terms of SSE and SAD and EM has slightly better results in terms of DBP for the nonlinear model. The comparison of the results of the various Muskingum models indicates that all nonlinear models have better performance than the linear model in terms of SSE and SAD. The improvement of the performance of the nonlinear models is at least 48% (i.e., 92% decreasing SSE value). Between nonlinear models, the NL5 has the best results in terms of SSE and SAD, while DBP of the NL1 has the lowest value. However, there is no significant difference between the performance of the NL3 and the NL5.

### *Second Case Study: Single-Peak Flood Hydrograph*

Wilson (1974) flood data has extensively been used for the evaluation of the lumped flood routing procedures, especially for direct routing (e.g., Easa 2014). Moreover, Das (2009) used this flood data for reverse flood routing by minimizing the normalized differences between observed and calculated inflows subject to satisfaction of the Muskingum routing equations. The relationship between storage volume and weighted flow is highly nonlinear as well-known in the previous studies (Vatankhah 2014). The optimal values of estimated parameters of proposed models and the corresponding evaluation criteria values are listed in Table 2. As it can be seen, the exponential parameter of the NL1 is 1.8551, which illustrates the nonlinearity of the relationship between storage volume and weighted flow.

For the comparison purpose, the results of Das (2009) are considered. The routed upstream hydrographs of the LN and the NL1 together with the observed values are shown in Fig. 3. The results of Das (2009) for the LN are SSE = 3,624, SAD = 212, DBP = 19.5, and DBTP = 2 with $X = 0.3396$ and $K = 22.001$, and for the NL1 were SSE = 330, SAD = 55, DPO = 4.2, and DBTP = 1 with $X = 0.2917$, $K = 0.0852$, and $m_1 = 2.2626$. It can be concluded that the result of the LN of the present methodology is better than the result of the LN by Das (2009) and the performance of the NL1 is better than the result of the NL1 by Das (2009) in terms of the evaluation criteria. The improvement of the performances of the LN and the NL1 are 38% (i.e., 62% decreasing SSE value) and 31% (i.e., 45% decreasing SSE value). Such improvement was achieved against the proposed methodology of Das (2009), which solves a system of equations with the implicit numerical method, whereas the present methodology uses an explicit method without any system of equations.

**Table 2.** Estimated optimal parameter and evaluation criteria values of Muskingum models for single-peak flood data

| Routing parameters or criteria | Storage model | | | | | | | | Das (2009) | |
|---|---|---|---|---|---|---|---|---|---|---|
| | LN | | NL1 | | | | | | | |
| | EM | FORK | EM | FORK | NL2 | NL3 | NL4 | NL5 | LN | NL1 |
| $K$ | 29.4896 | 27.8557 | 0.1565 | 0.9139 | 120.0604 | 122.9940 | 0.5271 | 0.9136 | 22.001 | 0.0852 |
| $X$ | 0.3877 | 0.4463 | 0.3564 | 0.2872 | 0.4701 | 0.5000 | 0.3488 | 0.1794 | 0.3396 | 0.2917 |
| $m_1$ | — | — | 2.1368 | 1.8551 | 0.7804 | 0.7605 | 0.6703 | 0.6502 | — | 2.2626 |
| $m_2$ | — | — | — | — | — | 0.7834 | 2.9291 | 0.4940 | — | — |
| $C$ | — | — | — | — | — | — | — | 3.4681 | — | — |
| SSE ($m^3 \cdot s^{-1}$) | 2,311 | 2,237 | 313 | **228** | 3,669 | 3,576 | 470 | 463 | 3,624 | 330 |
| SAD ($m^3 \cdot s^{-1}$) | 190 | 184 | 62 | 56 | 209 | 208 | 82 | 81 | 212 | **55** |
| DBP ($m^3 \cdot s^{-1}$) | 12.5 | 12.4 | 3.1 | **1.7** | 25.2 | 24.4 | 7.2 | 7.2 | 19.5 | 4.2 |
| DBTP | 1 | 1 | 1 | 1 | 2 | 2 | **0** | **0** | 2 | 1 |

Note: Bold values indicate the minimum value (better performance) among different approaches.

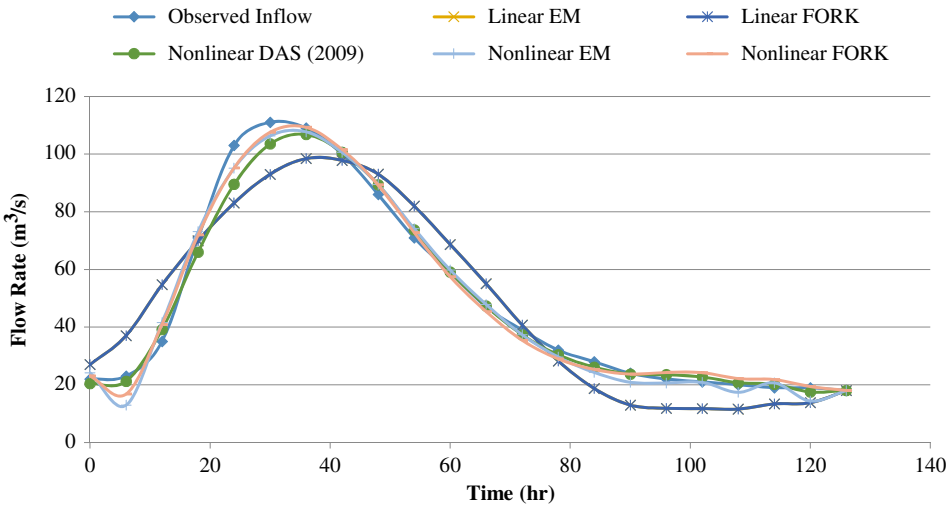


**Fig. 3.** Comparison of routed upstream hydrographs of the present study and the Das (2009) for single-peak flood data.

The EM and FORK have almost similar performances for LN, while FORK has 27% better results than EM in term of SSE value for the NL1. The comparison among used storage equations indicates that the NL1, NL4, and NL5 have better accuracy than the LN by at least 79% improvement in term of SSE value while the LN has better performance than the NL2 and NL3. Between nonlinear models, the NL1 has the best results in terms of SSE, SAD, and DBP. However, the accuracy of the NL4 and NL5 are an acceptable level.

### *Third Case Study: Double-Peak Flood Hydrograph*

Saghafian et al. (2015) used a double-peak flood hydrograph in a rectangular channel with length of 4,500 m, a bed width of 50 m, a bed slope of 0.01, and a Manning roughness coefficient of 0.025. They used the kinematic wave approach using a time step of 3 min for numerical simulation. The relationship between storage volume and weighted flow is relatively linear (Saghafian et al. 2015).

In Table 3, flood routing parameters of different models are presented. The evaluation criteria values of used models and the corresponding results of Saghafian et al. (2015) are also presented in Table 3. As seen, the performance of all Muskingum models are much better than the result of the kinematic wave (KW) model coupled with a GA of Saghafian et al. (2015) in terms of all performance evaluation criteria. The improvement of the performance of the Muskingum models is at least 29% (i.e., 41% decreasing SSE value) for the linear model, and the most improvement of the accuracy is 37% (i.e., 58% decreasing SSE value) for the NL5 in term of SSE value. Moreover, the drawback of the simulation result of the triangular flood data of Saghafian et al. (2015) (i.e., simulating a nonsmooth hydrograph) can also be observed for the results of the double-peak flood data using KW-GA methodology, while smooth curves are generated using all the Muskingum models in this study (Fig. 4).

The comparison of the results of the EM and FORK for the LN and NL1 indicates that both numerical schemes have the same performance for the linear model, while the EM has slightly better accuracy than the FORK for the nonlinear model. The comparison among used storage equations indicates that the accuracy of the LN is almost similar to nonlinear models, and for the best results of the nonlinear models, the improvement of the accuracy of the NL5 is about 10% than the LN. It can be said that there is no significant difference between the performances of different Muskingum models for this particular flood data.

### *Fourth Case Study: Multipeak Flood Hydrograph*

Barati et al. (2012) used a multipeak flood event of Karoon River, located in Ahvaz, Iran, for the direct flood routing. The considered reach has a length of 61 km, a bed width of 277 m, an average bed slop of 0.00011, and Manning's roughness coefficient of 0.025. The estimated optimal flood routing parameters of different models are summarized in Table 4. It is notable that the result of the LN

**Table 3.** Estimated optimal parameter and evaluation criteria values of Muskingum models for double-peak flood hydrograph

| Routing parameters or criteria | Storage model | | | | | | | | Saghafian et al. (2015) |
|---|---|---|---|---|---|---|---|---|---|
| | LN | | NL1 | | | | | | |
| | EM | FORK | EM | FORK | NL2 | NL3 | NL4 | NL5 | |
| $K$ | 12.9757 | 26.7943 | 1.0039 | 10.7288 | 29.9110 | 60.5555 | 11.2458 | 200.00 | — |
| $X$ | 0.3006 | 0.1961 | 0.3107 | 0.2040 | 0.1952 | 0.1013 | 0.2094 | 0.0042 | — |
| $m_1$ | — | — | 1.4145 | 1.1429 | 0.9832 | 0.9739 | 0.9741 | 0.9104 | — |
| $m_2$ | — | — | — | — | — | 0.8524 | 1.1613 | 0.3307 | — |
| $C$ | — | — | — | — | — | — | — | 1.9433 | — |
| SSE ($m^3 \cdot s^{-1}$) | 967 | 967 | 896 | 943 | 966 | 963 | 938 | **866** | 1,368 |
| SAD ($m^3 \cdot s^{-1}$) | 124 | 124 | 122 | 127 | 125 | 122 | 127 | **117** | 858 |
| DBP ($m^3 \cdot s^{-1}$) | 7.6 | 7.6 | 8.3 | 8.5 | 7.5 | **7.0** | 8.4 | 7.2 | 45.6 |
| DBTP | **0** | **0** | **0** | **0** | **0** | **0** | **0** | **0** | 4 |

Note: Bold values indicate the minimum value (better performance) among different approaches.

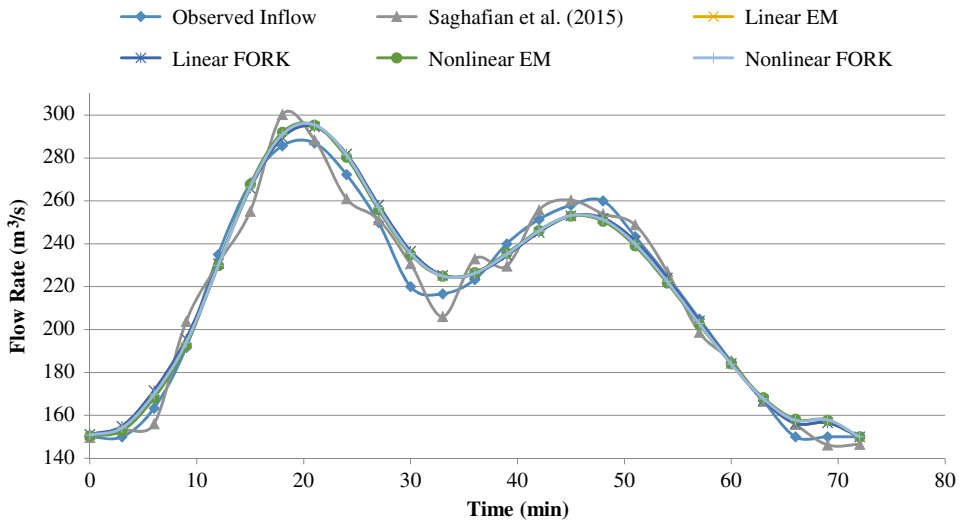


**Fig. 4.** Comparison of routed upstream hydrographs of the present study and Saghafian et al. (2015) for two-peak flood data.

**Table 4.** Estimated optimal parameter and evaluation criteria values of Muskingum models for multipeak flood event

| Routing parameters or criteria | Storage model | | | | | |
|---|---|---|---|---|---|---|
| | LN | NL1 | NL2 | NL3 | NL4 | NL5 |
| $X$ | — | 0.5000 | 0.5000 | 0.5000 | 0.4992 | 0.4996 |
| $K$ | — | 93.2129 | 20.0000 | 399.9780 | 169.7692 | 387.3628 |
| $m_1$ | — | 0.4888 | 0.6785 | 0.3209 | 1.1130 | 5.4892 |
| $m_2$ | — | — | — | 5.0146 | 0.3720 | 4.9393 |
| $C$ | — | — | — | — | — | 0.0491 |
| SSE ($m^3 \cdot s^{-1}$) | — | 124,539 | 135,765 | 120,724 | 138,466 | **108,153** |
| SAD ($m^3 \cdot s^{-1}$) | — | 1,891 | 1,948 | 1,806 | 2,060 | **1,710** |

Note: Bold values indicate the minimum value (better performance) among different approaches.

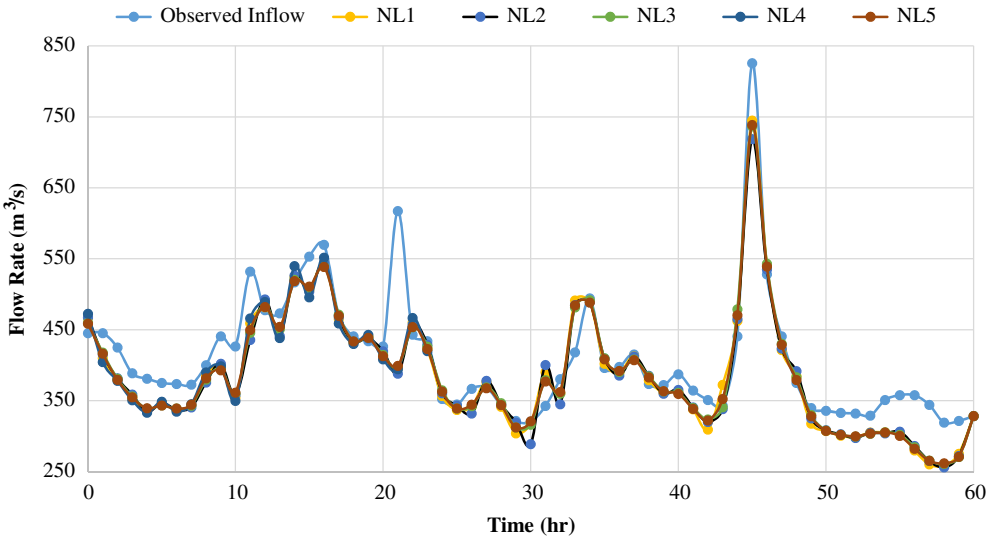


**Fig. 5.** Observed and simulated upstream flood hydrographs for the multipeak flood event.

model is not acceptable for such data and therefore it is not presented herein.

Inflow hydrographs of the different models using the FORK numerical scheme are compared with observed values in Fig. 5. It can be concluded that the results of developed models fairly followed the observed inflow hydrograph values. The different nonlinear Muskingum models can capture most of the peak flows.

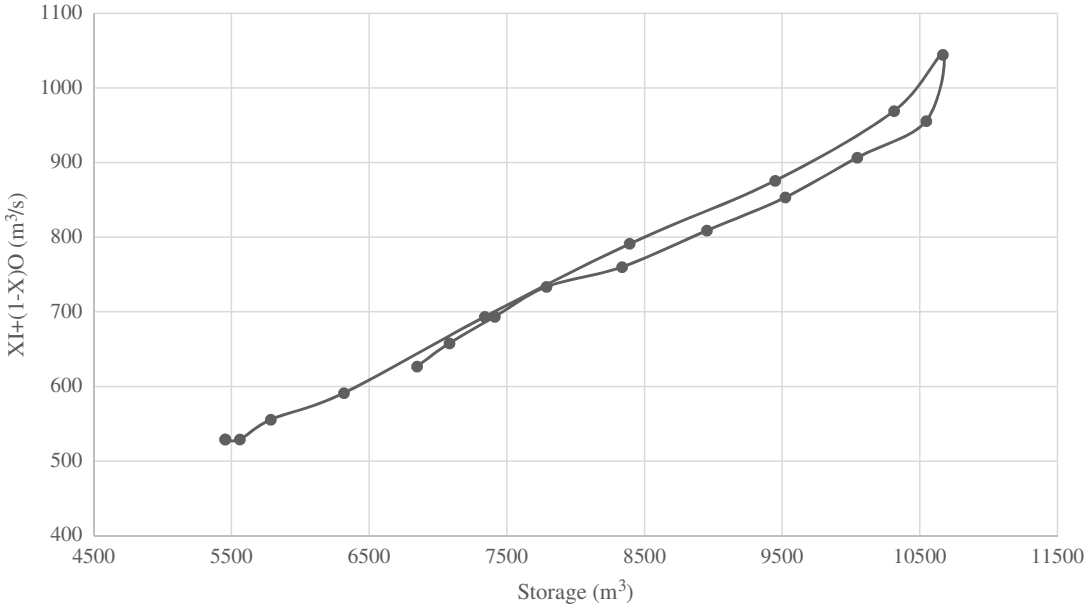


**Fig. 6.** Relationship between storage volume and weighted flow for single-peak flood event 1 of the Karoon River (used in calibration step).

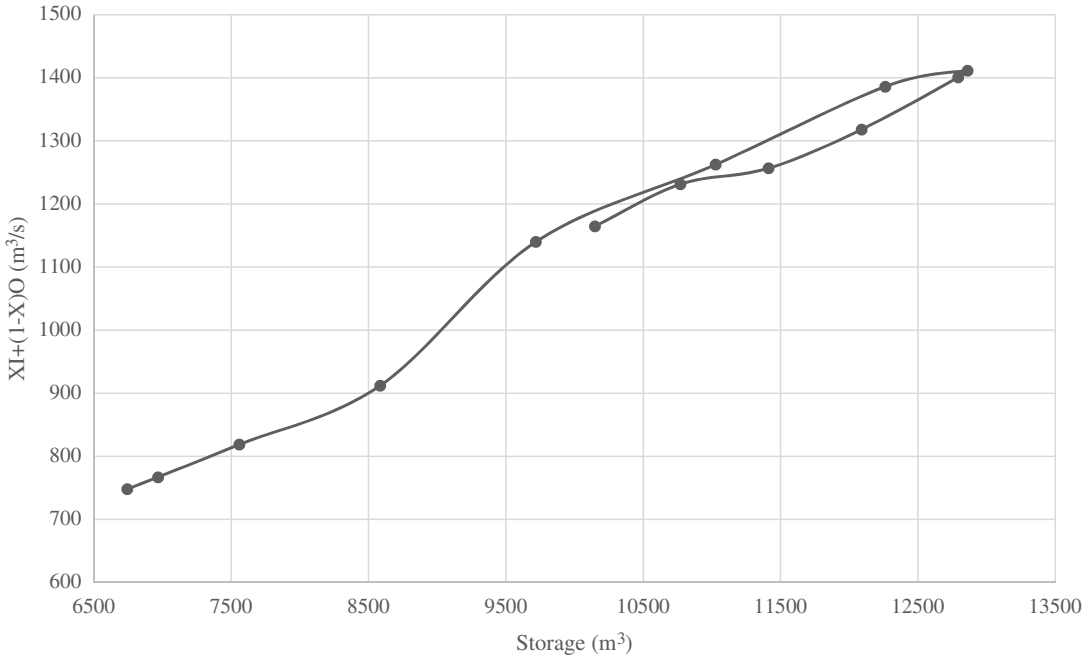


**Fig. 7.** Relationship between storage volume and weighted flow for single-peak flood event 2 of the Karoon River (used in validation step).

In Table 4, the values of SSE and SAD are also presented. It can be seen that the NL5 has the best results in terms of both SSE and SAD. The improvement of the performance of the NL5 is in the range of 10%–21% in terms of SSE. Nevertheless, all the nonlinear Muskingum models have acceptable accuracy and promising results for the simulation of the multipeak hydrographs.

### *Validation of the Model*

Two single-peak flood events of Karoon River (Barati et al. 2012) were considered to calibrate and validate the proposed models. The study reach adopted for this exercise is the reach between two gauging stations along the Karoon River (Molasani is the upstream gauging station and Ahwaz is the downstream gauging station). The length, width, and bed slope of Karoon River are 61 km, 277 m, and 0.11 m/km, respectively. The relationships between storage volumes and weighted flows for the two events are shown in Figs. 6 and 7.

The optimal parameters adopted for calibration and performance evaluation criteria values for the different Muskingum models are presented in Table 5. The corresponding results in terms of hydrographs are presented in Fig. 8. As presented in Table 5, the NL4 model has the best accuracy in terms of SSE; the NL4 and NL5 models have the best accuracy in terms of SAD, and the NL5 has the best result in term of DBP.

**Table 5.** Estimated parameters and evaluation criteria values of Muskingum models for the Karoon River in the calibration step

| Routing parameters or criteria | Storage model | | | | | |
|---|---|---|---|---|---|---|
| | LN | NL1 | NL2 | NL3 | NL4 | NL5 |
| $X$ | 0.3414348 | 0.3389439 | 0.4000 | 0.0002 | 0.3176 | 0.4815 |
| $K$ | 20.15775 | 28.35551 | 0.2060 | 150.0000 | 5.8325 | 2.3402 |
| $m_1$ | — | 0.956129 | 1.6000 | 1.6982 | 1.9265 | 1.7613 |
| $m_2$ | — | — | — | 0.6993 | 0.6015 | 1.8687 |
| $C$ | — | — | — | — | — | 0.7037 |
| SSE ($m^3 \cdot s^{-1}$) | 41,226 | 41,191 | 36,354 | 25,176 | **15,414** | 18,008 |
| SAD ($m^3 \cdot s^{-1}$) | 620 | 620 | 581 | 484 | **399** | **399** |
| DBP ($m^3 \cdot s^{-1}$) | 51.0 | 51.0 | 58.1 | 25.9 | 22.5 | **12.8** |
| DBTP | **0** | 1 | **0** | **0** | 1 | 1 |

Note: Bold values indicate the minimum value (better performance) among different approaches.

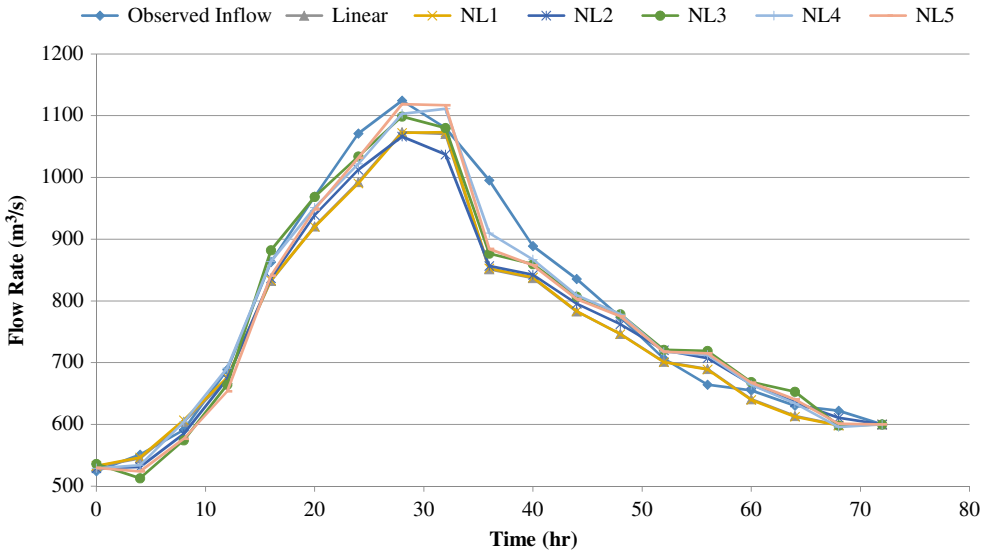


**Fig. 8.** Comparison of results of reverse flood routing for the Karoon River in the calibration step.

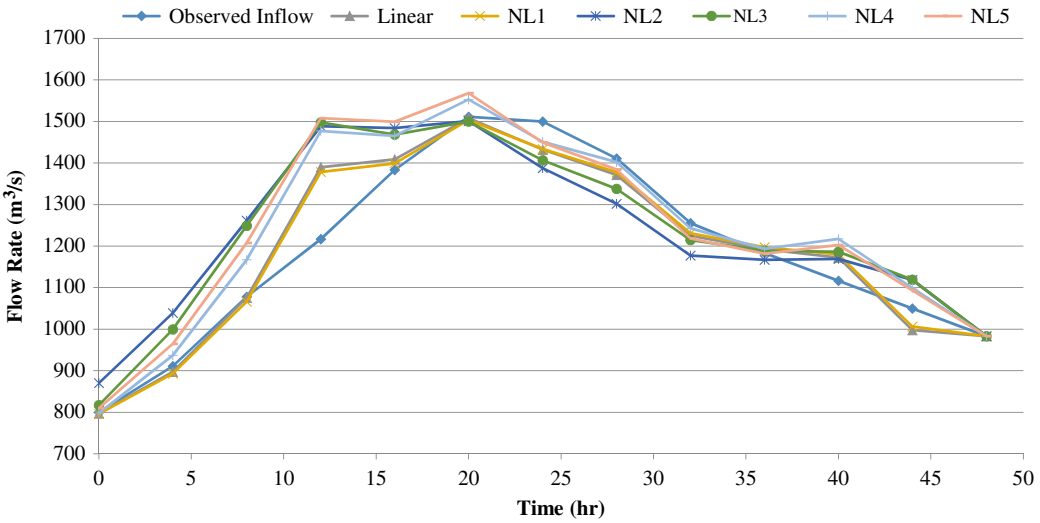


**Fig. 9.** Comparison of results of reverse flood routing for the Karoon River in the validation step.

The parameters adopted for validation are similar to those presented in Table 5 in conjunction with Fig. 7. The corresponding results in terms of hydrographs and differences between observed and routed flows are presented in Figs. 9 and 10, respectively. As presented in Table 6, the NL1 model in terms of SSE and SAD criteria, followed by the LN model in terms of DBP. It should be noted that, in the present study, only one flood event was used for calibration of the routing parameters. If more flood events are

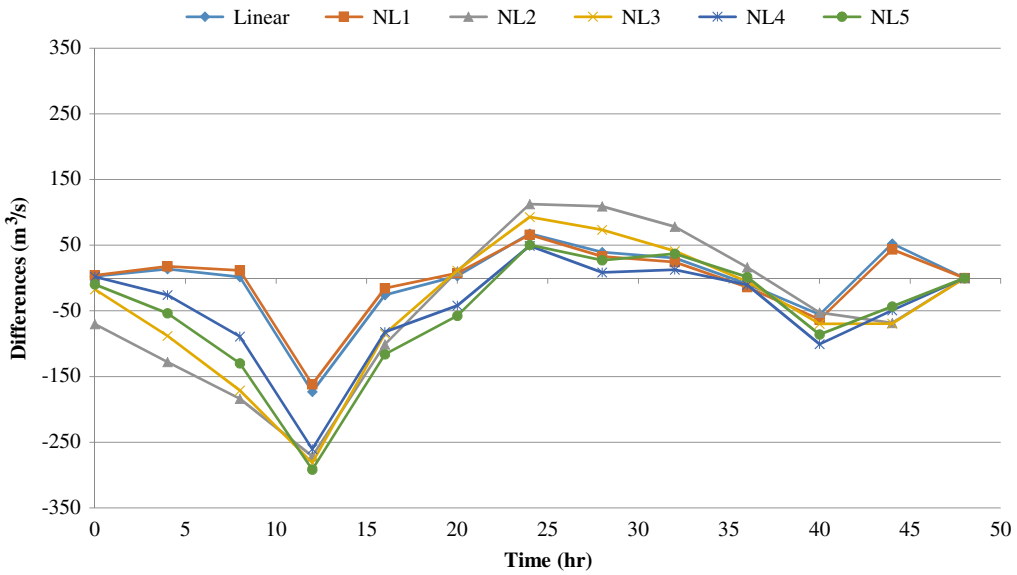


**Fig. 10.** Comparison of differences between observed and routed flows for the Karoon River in the validation step.

**Table 6.** Evaluation criteria values for Muskingum models for the Karoon River in the validation step

| | Storage model | | | | | |
|---|---|---|---|---|---|---|
| Criteria | LN | NL1 | NL2 | NL3 | NL4 | NL5 |
| SSE ($m^3 \cdot s^{-1}$) | 43,810 | **39,134** | 177,613 | 149,204 | 100,199 | 135,600 |
| SAD ($m^3 \cdot s^{-1}$) | 475 | **463** | 1,202 | 1,006 | 732 | 904 |
| DBP ($m^3 \cdot s^{-1}$) | **3.2** | 7.5 | 10.3 | 11.2 | 42.0 | 57.4 |
| DBTP | **0** | **0** | **0** | **0** | **0** | **0** |

Note: Bold values indicate the minimum value (better performance) among different approaches.

available for the calibration process, more accurate results can be achieved in the validation step.

## Conclusions

In this study, reverse flood routing is implemented by application of the EM and FORK numerical solution methods in connection with the SCE optimization algorithm for all six storage equations of the Muskingum flood routing model. The EM and FORK numerical schemes are advantageous in that these models are explicit and numerically stable. The advantages of the SCE optimization algorithm are such that it does not need an initial guess, it has low sensitivity to the parameter change, and is highly convergent. A triangular, a single-peak, a double-peak, and multipeak flood hydrographs were used for model calibration, and a real case event was used for model validation. The application of the proposed methodology for the triangular, the single-peak, and the two-peak flood hydrographs improved 82%, 31%, and 30%, respectively, than the best existing results. The practical applicability of the proposed approach is also demonstrated in real river systems for both calibration and validation steps.

## Data Availability Statement

Some or all data, models, or code that support the findings of this study are available from the corresponding author upon request.

## Acknowledgments

The authors appreciatively acknowledge the valuable comments offered by the editors and anonymous reviewers in improving the technical contents of this paper.

## References

Abdulwahid, M. H., and K. N. Kadhim. 2013. "Application of inverse routing methods to Euphrates river (IRAQ)." *Int. J. Civ. Eng. Technol.* 4 (1): 97–109.

Akbari, G. H., A. H. Nezhad, and R. Barati. 2012. "Developing a model for analysis of uncertainties in prediction of floods." *J. Adv. Res.* 3 (1): 73–79. https://doi.org/10.1016/j.jare.2011.04.004.

Artichowicz, W., and R. Szymkiewicz. 2009. "Inverse integration of the open channel flow equations." In Vol. I of *Proc., 11th International Symp. on Water Management and Hydraulic Engineering*, 89–96. Skopje, Macedonia: Univ. of Skopje.

Ayvaz, M. T., and G. Gurarslan. 2017. "A new partitioning approach for nonlinear Muskingum flood routing models with lateral flow contribution." *J. Hydrol.* 553 (Oct): 142–159. https://doi.org/10.1016/j.jhydrol.2017.07.050.

Badfar, M. 2015. "Developing a model for reverse flood routing in rivers." M.Sc. thesis, Dept. of Civil Engineering, Univ. of Sistan and Baluchestan.

Barati, R. 2011. "Parameter estimation of nonlinear Muskingum models using Nelder-Mead simplex algorithm." *J. Hydrol. Eng.* 16 (11): 946–954. https://doi.org/10.1061/(ASCE)HE.1943-5584.0000379.

Barati, R. 2013. "Application of excel solver for parameter estimation of the nonlinear Muskingum models." *KSCE J. Civ. Eng.* 17 (5): 1139–1148. https://doi.org/10.1007/s12205-013-0037-2.

Barati, R., S. Rahimi, and G. H. Akbari. 2012. "Analysis of dynamic wave model for flood routing in natural rivers." *Water Sci. Eng.* 5 (3): 243–258.

Battjes, J. A., and R. J. Labeur. 2017. *Unsteady flow in open channels*. New York: Cambridge University Press.

Bruen, M., and J. C. I. Dooge. 2007. "Harmonic analysis of the stability of reverse routing in channels." *Hydrol. Earth Syst. Sci. Discuss.* 11 (1): 559–568.

Brutsaert, W. 2005. *Hydrology: An introduction*. New York: Cambridge University Press.

Cheng, S. J., and R. Y. Wang. 2002. "An approach for evaluating the hydrological effects of urbanization and its application." *Hydrol. Process.* 16 (7): 1403–1418. https://doi.org/10.1002/hyp.350.

Chow, V. 1959. *Open channel hydraulics*. New York: McGraw-Hill.

Chow, V. T., D. R. Maidment, and L. W. Mays. 1988. *Applied hydrology*, 572. Singapore: McGraw-Hill.

Contractor, D. N., and J. W. Jenson. 2000. "Simulated effect of vadose infiltration on water levels in the Northern Guam Lens Aquifer." *J. Hydrol.* 229 (3–4): 232–254. https://doi.org/10.1016/S0022-1694(00)00157-8.

Das, A. 2009. "Reverse stream flow routing by using Muskingum models." *Sadhana* 34 (3): 483–499. https://doi.org/10.1007/s12046-009-0019-8.

Dooge, J., and M. Bruen. 2005. "Problems in reverse routing." *Acta Geophys. Pol.* 53 (4): 357.

D'Oria, M., P. Mignosa, and M. G. Tanda. 2012. "Reverse level pool routing: Comparison between a deterministic and a stochastic approach." *J. Hydrol.* 470 (Nov): 28–35. https://doi.org/10.1016/j.jhydrol.2012.07.045.

D'Oria, M., P. Mignosa, and M. G. Tanda. 2014. "Bayesian estimation of inflow hydrographs in ungauged sites of multiple reach systems." *Adv. Water Resour.* 63 (Jan): 143–151. https://doi.org/10.1016/j.advwatres.2013.11.007.

D'Oria, M., and M. G. Tanda. 2012. "Reverse flow routing in open channels: A Bayesian geostatistical approach." *J. Hydrol.* 460 (Aug): 130–135. https://doi.org/10.1016/j.jhydrol.2012.06.055.

Duan, Q. 2003. "Global optimization for watershed model calibration." *Calibration Watershed Models* 6: 89–104.

Duan, Q., V. Gupta, and S. Sorooshian. 1993. "Shuffled complex evolution approach for effective and efficient global minimization." *J. Optim. Theory Appl.* 76 (3): 501–521. https://doi.org/10.1007/BF00939380.

Duan, Q., S. Sorooshian, and V. Gupta. 1992. "Effective and efficient global optimization for conceptual rainfall-runoff models." *Water Resour. Res.* 28 (4): 1015–1031. https://doi.org/10.1029/91WR02985.

Duan, Q., S. Sorooshian, and V. Gupta. 1994. "Optimal use of the SCE-UA global optimization method for calibrating watershed models." *J. Hydrol.* 158 (3–4): 265–284. https://doi.org/10.1016/0022-1694(94)90057-4.

Easa, S. M. 2014. "New and improved four-parameter non-linear Muskingum model." *Proc. Inst. Civ. Eng.* 167 (5): 288.

Easa, S. M., R. Barati, H. Shahheydari, E. J. Nodoshan, and T. Barati. 2014. "Discussion: New and improved four-parameter non-linear Muskingum model." *Water Manage.* 167 (10): 612–615.

Eckhardt, K., and J. G. Arnold. 2001. "Automatic calibration of a distributed catchment model." *J. Hydrol.* 251 (1–2): 103–109. https://doi.org/10.1016/S0022-1694(01)00429-2.

Ehteram, M., et al. 2018. "Improving the Muskingum flood routing method using a hybrid of particle swarm optimization and bat algorithm." *Water* 10 (6): 807.

Eli, R. N., J. M. Wiggert, and D. N. Contractor. 1974. "Reverse flow routing by the implicit method." *Water Resour. Res.* 10 (3): 597–600. https://doi.org/10.1029/WR010i003p00597.

Eusuff, M. M., and K. E. Lansey. 2004. "Optimal operation of artificial groundwater recharge systems considering water quality transformations." *Water Resour. Manage.* 18 (4): 379–405. https://doi.org/10.1023/B:WARM.0000048486.46046.ee.

Gavilan, G., and M. H. Houck. 1985. "Optimal Muskingum River routing." In *Proc., Computer Applications in Water Resources*, 1294–1302. Reston, VA: ASCE.

Gill, M. 1978. "Flood routing by Muskingum method." *J. Hydrol.* 36 (3–4): 353–363. https://doi.org/10.1016/0022-1694(78)90153-1.

Gupta, H. V., S. Sorooshian, and P. O. Yapo. 1999. "Status of automatic calibration for hydrologic models: Comparison with multilevel expert calibration." *J. Hydrol. Eng.* 4 (2): 135–143. https://doi.org/10.1061/(ASCE)1084-0699(1999)4:2(135).

Kang, L., L. Zhou, and S. Zhang. 2017. "Parameter estimation of two improved nonlinear Muskingum models considering the lateral flow using a hybrid algorithm." *Water Resour. Manage.* 31 (14): 4449–4467. https://doi.org/10.1007/s11269-017-1758-7.

Koussis, A. D. 2009. "Assessment and review of the hydraulics of storage flood routing 70 years after the presentation of the Muskingum method." *Hydrol. Sci. J.* 54 (1): 43–61. https://doi.org/10.1623/hysj.54.1.43.

Koussis, A. D., K. Mazi, S. Lykoudis, and A. A. Argiriou. 2012. "Reverse flood routing with the inverted Muskingum storage routing scheme." *Nat. Hazards Earth Syst. Sci.* 12 (1): 217–227.

McCarthy, G. 1938. "The unit hydrograph and flood routing North Atlantic division." In *Proc., Conf. of North Atlantic Division, US Army Corps of Engineers*. Providence, RI: US Army Corps of Engineers.

Mertens, J., H. Madsen, L. Feyen, D. Jacques, and J. Feyen. 2004. "Including prior information in the estimation of effective soil parameters in unsaturated zone modeling." *J. Hydrol.* 294 (4): 251–269. https://doi.org/10.1016/j.jhydrol.2004.02.011.

Niazkar, M., and S. H. Afzali. 2017. "New nonlinear variable-parameter Muskingum models." *KSCE J. Civ. Eng.* 21 (7): 2958–2967. https://doi.org/10.1007/s12205-017-0652-4.

Perumal, M., and B. Sahoo. 2007. "Applicability criteria of the variable parameter Muskingum stage and discharge routing methods." *Water Resour. Res.* 43 (5): 1–20.

Price, R. K., W. A. Y. S. Fernando, and D. P. Solomatine. 2006. "Inverse modeling for flood propagation." In *Proc., 7th Int. Conf. on Hydroinformatics*. Nice, France: Research Pub.

Sadeghi, S. H., and J. K. Singh. 2010. "Derivation of flood hydrographs for ungauged upstream subwatersheds using a main outlet hydrograph." *J. Hydrol. Eng.* 15 (12): 1059–1069. https://doi.org/10.1061/(ASCE)HE.1943-5584.0000275.

Saghafian, B., M. H. Jannaty, and N. Ezami. 2015. "Inverse hydrograph routing optimization model based on the kinematic wave approach." *Eng. Optim.* 47 (8): 1031–1042. https://doi.org/10.1080/0305215X.2014.941289.

Sivapragasam, C., R. Maheswaran, and V. Venkatesh. 2008. "Genetic programming approach for flood routing in natural channels." *Hydrol. Processes Int. J.* 22 (5): 623–628. https://doi.org/10.1002/hyp.6628.

Sorooshian, S., Q. Duan, and V. K. Gupta. 1993. "Calibration of rainfall-runoff models: Application of global optimization to the Sacramento soil moisture accounting model." *Water Resour. Res.* 29 (4): 1185–1194. https://doi.org/10.1029/92WR02617.

Spada, E., M. Sinagra, T. Tucciarelli, S. Barbetta, T. Moramarco, and G. Corato. 2017. "Assessment of river flow with significant lateral inflow through reverse routing modeling." *Hydrol. Process.* 31 (7): 1539–1557. https://doi.org/10.1002/hyp.11125.

Szymkiewicz, R. 1993. "Solution of the inverse problem for the Saint Venant equations." *J. Hydrol.* 147 (1–4): 105–120. https://doi.org/10.1016/0022-1694(93)90077-M.

Szymkiewicz, R. 2010. Vol. 83 of *Numerical modeling in open channel hydraulics*. New York: Springer.

Tung, Y. 1985. "River flood routing by nonlinear Muskingum method." *J. Hydraul. Eng.* 111 (12): 1447–1460. https://doi.org/10.1061/(ASCE)0733-9429(1985)111:12(1447).

van Griensven, A., and W. Bauwens. 2003. "Concepts for river water quality processes for an integrated river basin modeling." *Water Sci. Technol.* 48 (3): 1–8. https://doi.org/10.2166/wst.2003.0145.

Vatankhah, A. R. 2014. "Evaluation of explicit numerical solution methods of the Muskingum model." *J. Hydrol. Eng.* 19 (8): 06014001. https://doi.org/10.1061/(ASCE)HE.1943-5584.0000978.

Vatankhah, A. R. 2015. "Discussion of 'application of excel solver for parameter estimation of the nonlinear Muskingum models' by Reza

Barati." *KSCE J. Civ. Eng.* 19 (1): 332–336. https://doi.org/10.1007/s12205-014-1422-1.
Wilson, E. M. 1974. *Engineering hydrology.* Hampshire, UK: MacMillan.
Yapo, P. O., H. V. Gupta, and S. Sorooshian. 1996. "Automatic calibration of conceptual rainfall-runoff models: Sensitivity to calibration data." *J. Hydrol.* 181 (1–4): 23–48. https://doi.org/10.1016/0022-1694(95)02918-4.
Zoppou, C. 1999. "Reverse routing of flood hydrographs using level pool routing." *J. Hydrol. Eng.* 4 (2): 184–188. https://doi.org/10.1061/(ASCE)1084-0699(1999)4:2(184).
Zucco, G., G. Tayfur, and T. Moramarco. 2015. "Reverse flood routing in natural channels using genetic algorithm." *Water Resour. Manage.* 29 (12): 4241–4267. https://doi.org/10.1007/s11269-015-1058-z.